Contribution from the Department of Chemistry, University of Houston, Houston, Texas 77004

# Microvoltammetry and in Situ FTIR, ESR, and UV–Visible Spectroelectrochemical Studies of (TPP)Co(NO) Oxidation/Reduction in Dichloromethane

K. M. Kadish,* X. H. Mu, and X. Q. Lin

*Received November 10, 1987*

The techniques of in situ ESR, FTIR, and UV–visible spectroelectrochemistry were combined with microvoltammetry and classical electrochemical techniques in order to elucidate the prevailing mechanism of electron transfer for (TPP)Co(NO) (where TPP is the dianion of tetraphenylporphyrin) in $CH_2Cl_2$. Five reversible oxidation/reduction reactions can be observed for (TPP)Co(NO) at a Pt microelectrode of 25-μm diameter. Two oxidations occur at 1.01 and 1.25 V, while three reductions occur at −1.18, −1.75, and −2.30 V. Each oxidation and reduction was examined with respect to the site of electron transfer and to the fate of the NO group on the time scales of thin-layer cyclic voltammetry and bulk controlled-potential electrolysis. The NO group remains coordinated to the cobalt center after electrooxidation of (TPP)Co(NO), and a shift in NO vibration from 1684 to 1726 $cm^{-1}$ is observed upon going from (TPP)Co(NO) to $[(TPP)Co(NO)]^+$. In situ ESR and thin-layer spectroelectrochemistry indicate that the electron is abstracted from the porphyrin π ring system during the first oxidation, and an $A_{2u}$ radical is assigned on the basis of ESR data. The NO ligand dissociates from the central cobalt ion after the other four electrode reactions of (TPP)Co(NO). A comparison between electrochemical results at a microelectrode and at a conventional electrode is given, and an overall scheme for oxidation/reduction of (TPP)Co(NO) is presented.

## Introduction

Several chemical[1–3] and electrochemical[4–12] studies involving metalloporphyrins and related macrocycles coordinated by nitrosyl ligands have been carried out with the aim of understanding the multielectron reduction of nitrite to ammonia catalyzed by enzymes. The singly oxidized species are generally stable in noncoordinating media, and complexes of $[(OEP)Co(NO)]^+$, $[(OEC)Co(NO)]^+$, and $[(OEiBC)Co(NO)]^+$ have been spectroscopically identified.[7,13]

This paper reports a detailed study of the oxidation and reduction of (TPP)Co(NO) in $CH_2Cl_2$. Preliminary voltammetric data for formation of $[(TPP)Co(NO)]^+$ and $[(TPP)Co(NO)]^-$ have been reported,[9] but a spectroscopic characterization of these species has never been published. There is also no information on the doubly oxidized and doubly reduced $[(TPP)Co(NO)]^{2+}$ and $[(TPP)Co(NO)]^{2-}$ complexes.

(TPP)Co(NO) can undergo up to two oxidations and three reductions in $CH_2Cl_2$. These reactions are given by eq 1–5. The

$$(TPP)Co(NO) \rightleftarrows [(TPP)Co(NO)]^+ + e^- \quad (1)$$

$$[(TPP)Co(NO)]^+ \rightleftarrows [(TPP)Co(NO)]^{2+} + e^- \quad (2)$$

$$(TPP)Co(NO) + e^- \rightleftarrows [(TPP)Co(NO)]^- \quad (3)$$

$$[(TPP)Co(NO)]^- + e^- \rightleftarrows [(TPP)Co(NO)]^{2-} \quad (4)$$

$$[(TPP)Co(NO)]^{2-} + e^- \rightleftarrows [(TPP)Co(NO)]^{3-} \quad (5)$$

first four reactions occur at room temperature, while reaction 5 in only observed by cyclic voltammetry at high potential scan rates or at low temperature.

In this study, the techniques of ESR, IR, and UV–visible spectroelectrochemistry are combined with microvoltammetry and classical electrochemistry in order to monitor each of the above electron transfers in $CH_2Cl_2$. The NO bands are quite well-defined by infrared spectroscopy and thus provide diagnostic criteria for evaluating the extent of NO binding to electrooxidized and/or electroreduced (TPP)Co(NO). The supporting electrolyte, tetrabutylammonium perchlorate (TBAP), and solvent, $CH_2Cl_2$, have no interfering absorbances between 1500 and 1950 $cm^{-1}$, and this also provides an opportunity to study the vibrations of bound NO in this solvent/supporting electrolyte mixture.

## Experimental Section

**Instrumentation and Procedures.** A homemade three-electrode cell was used for both conventional and microvoltammetric studies. The latter experiments were carried out in a well-grounded Faraday cage by using a homemade potentiostat that was driven by a PAR Model 175 universal programmer. A Textronic Model 5111 storage oscilloscope was used to record current–voltage curves. Conventional cyclic voltammograms were obtained with a PAR Model 174A polarographic analyzer and an Omnigraphic 2000 X-Y recorder. A platinum electrode with surface area of 0.8 $mm^2$ was used as the working electrode. A saturated calomel electrode (SCE) was used as the reference electrode and was separated from the bulk solution by a fritted-glass bridge. The auxiliary electrode was a large surface area platinum wire. A 25-μm–diameter platinum electrode served as the working electrode for microvoltammetry, while a large surface area platinum electrode was used as the auxiliary electrode. The reference electrode was Ag/AgCl with saturated KCl (which is 39 mV negative of a standard calomel electrode), and all potentials are reported as volts vs SCE. High-purity $N_2$ was used to deaerate the solution and to keep a positive gas pressure above the solution during the experiment.

Infrared measurements were carried out with an IBM 32 FTIR spectrometer and a light-transparent spectroelectrochemical three-electrode IR cell that was constructed for use on this project.[14] The spectrum of $CH_2Cl_2$ containing 0.1 M TBAP was taken as the background spectrum in order to minimize matrix interferences, and the reference spectrum was that of neutral (unoxidized or unreduced) (TPP)Co(NO). Difference spectra were obtained after controlled-potential electrolysis at specific potentials. Positive absorbances in the spectra correspond to a product generated during electrolysis, while negative absorbances correspond to a disappearance of the reactant.

ESR experiments were carried out after in situ oxidation in a three-electrode ESR cell and spectral monitoring with an IBM ER 100D spectrometer. UV–visible spectra were taken during electrolysis in a vacuum-tight thin-layer spectroelectrochemical cell that has a doublet platinum gauze working electrode. The design of the thin-layer UV–visible cell is described in the literature.[15] A Tracor Northern TN-1710 multichannel analyzer and a TN-1710-24 floppy disk system were used to record the spectra.

**Chemicals.** (TPP)Co(NO) was prepared from (TPP)Co by using published methods.[3] Methylene chloride ($CH_2Cl_2$) (spectroanalyzed grade, Fisher Scientific Co.) was freshly distilled from $CaH_2$ before use. Tetrabutylammonium perchlorate (Fluka Chemical Co.) was used as

(1) Wayland, B. B.; Minkiewicz, J. V.; Abd-Elmageed, M. E. *J. Am. Chem. Soc.* **1974**, *96*, 2795.
(2) Wayland, B. B.; Minkiewicz, J. V. *J. Chem. Soc., Chem. Commun.* **1976**, 1015.
(3) Scheidt, W. R.; Hoard, J. L. *J. Am. Chem. Soc.* **1973**, *95*, 8281.
(4) Barley, M. H.; Takeuchi, K. J.; Meyer, T. J. *J. Am. Chem. Soc.* **1986**, *108*, 5876.
(5) Fernandes, J. B.; Feng, D. W.; Chang, A.; Keyser, A.; Ryan, M. D. *Inorg. Chem.* **1986**, *25*, 2606.
(6) Fujita, E.; Fajer, J. *J. Am. Chem. Soc.* **1983**, *105*, 6743.
(7) Fujita, E.; Chang, C. K.; Fajer, J. *J. Am. Chem. Soc.* **1985**, *107*, 7665.
(8) Lançon, D.; Kadish, K. M. *J. Am. Chem. Soc.* **1983**, *105*, 5610.
(9) Kelly, S.; Lançon, D.; Kadish, K. M. *Inorg. Chem.* **1984**, *23*, 1451.
(10) Feng, D.; Ryan, M. D. *Inorg. Chem.* **1987**, *26*, 2480.
(11) Olson, L. W.; Schaefer, D.; Lançon, D.; Kadish, K. M. *J. Am. Chem. Soc.* **1982**, *104*, 2042.
(12) Newman, A. R.; French, A. N. *Inorg. Chim. Acta* **1987**, *129*, L37–L39.
(13) Abbreviations utilized for porphyrin dianions: OEP = octaethylporphyrin; OEC = octaethylchlorin; (OEiBC) = octaethylisobacteriochlorin; TPP = tetraphenylporphyrin.
(14) Kadish, K. M.; Lin, X. Q. *Proc. Beijing Conf. Exhib. Instrum. Anal.* **1987**, 1311.
(15) Lin, X. Q.; Kadish, K. M. *Anal. Chem.* **1985**, *57*, 1498.

0020-1669/88/1327-1489$01.50/0 

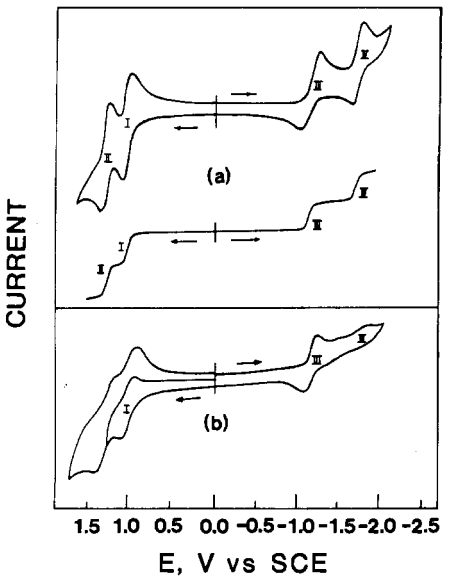


**Figure 1.** (a) Cyclic voltammogram (scan rate = 10 V/s) and steady-state voltammogram (scan rate 50 mV/s) of (TPP)Co(NO) at a microelectrode in $CH_2Cl_2$, 0.1 M TBAP. (b) Conventional cyclic voltammogram of (TPP)Co(NO) in $CH_2Cl_2$, 0.1 M TBAP (scan rate 0.1 V/s).

**Table I.** Half-Wave Potentials (V vs SCE) for Oxidation and Reduction of (TPP)Co(NO) and (TPP)Co in $CH_2Cl_2$, 0.1 M TBAP

| | oxidation | | | reduction | | |
|---|---|---|---|---|---|---|
| compd | 1st | 2nd | 3rd | 1st | 2nd | 3rd |
| (TPP)Co(NO) | 1.01 | 1.25 | | −1.18 | −1.75 | −2.30[a] |
| (TPP)Co | 0.78[b] | 0.97[b] | 1.16[b] | −0.85 | −2.05 | |

[a] −50 °C. [b] Taken from ref 15.

supporting electrolyte and was recrystallized from ethanol and dried in vacuo prior to use.

## Results and Discussion

**Electrooxidation of (TPP)Co(NO) at a Microelectrode.** Figure 1a shows a room-temeprature steady-state voltammogram and a cyclic voltammogram of (TPP)Co(NO) in $CH_2Cl_2$ at a 25-$\mu$m-diameter platinum electrode. The compound undergoes two reversible one-electron oxidations and two reversible one-electron reductions between +1.8 and −2.0 V. The oxidations are labeled as processes I and II and occur at $E_{1/2}$ = 1.01 and 1.25 V. These reactions are given by eq 1 and 2. The reductions are labeled as processes III and IV and occur at $E_{1/2}$ = −1.18 and −1.75 V. These reactions are given by eq 3 and 4. A third reduction (not shown in the Figure) is also observed at high potential scan rates or at low temperature. This reaction corresponds to the formation of $[(TPP)Co(NO)]^{3-}$ (eq 5) and occurs at $E_{1/2}$ = −2.30 V in $CH_2Cl_2$ at −50 °C. All of the potentials are summarized in Table I, which also lists values for oxidation and reduction of (TPP)Co under the same solution conditions.

The voltammogram of (TPP)Co(NO) from conventional cyclic voltammetry (Figure 1b) differs from that obtained at a microelectrode (Figure 1a). Both voltammograms show the same reversible one-electron oxidation at $E_{1/2}$ = 1.01 V (process I), but in conventional voltammetry this reaction is followed by a relatively broad peak at $E_p$ = 1.31 V. Differential pulse polarography of the same solution reveals that the second oxidation consists of two overlapping oxidation peaks at $E_p$ = 1.26 and 1.38 V.[9]

FTIR, ESR, and UV–visible spectral experiments (see later discussion) show that the first oxidation of (TPP)Co(NO) leads to a relatively stable $[(TPP)Co(NO)]^+$ cation radical but that NO is lost after generation of $[(TPP)Co(NO)]^{2+}$ on longer time scales. This loss of NO from $[(TPP)Co(NO)]^{2+}$ leads to $[(TPP)Co]^{2+}$ and $[(TPP)Co]^{3+}$, as shown by eq 6 and 7.

$$[(TPP)Co(NO)]^{2+} \rightarrow [(TPP)Co]^{2+} + NO \quad (6)$$

$$[(TPP)Co]^{2+} \rightleftarrows [(TPP)Co]^{3+} + e^- \quad (7)$$

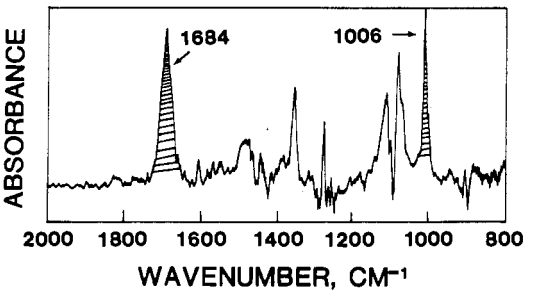


**Figure 2.** FTIR spectrum of neutral (TPP)Co(NO) in $CH_2Cl_2$, 0.1 M TBAP (vs the spectrum of $CH_2Cl_2$, 0.1 TBAP as background). The shaded peaks correspond to vibrations of bound NO (1684 $cm^{-1}$) and of the metalloporphyrin (1006 $cm^{-1}$).

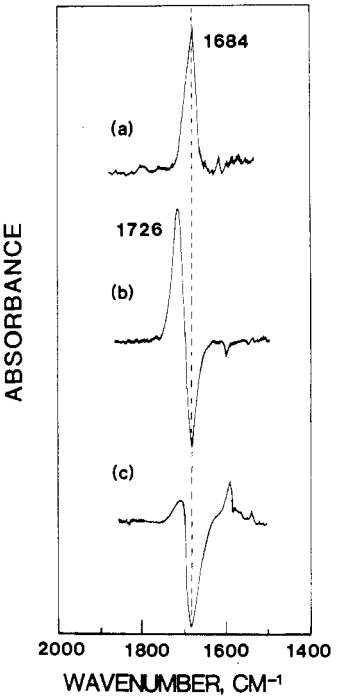


**Figure 3.** In situ FTIR difference spectra of (TPP)Co(NO): (a) before electrooxidation; (b) after controlled-potential oxidation at 1.10 V; (c) after controlled-potential oxidation at 1.40 V.

$[(TPP)Co]^{2+}$ is oxidized at $E_{1/2}$ = 1.16 V (see Table I) and thus, any $[(TPP)Co]^{2+}$ produced will be immediately converted to $[(TPP)Co]^{3+}$ at a potential of 1.25 V. This results in a larger peak current for the second oxidation of (TPP)Co(NO) by conventional voltammetry and the apparent overall conversion of $[(TPP)Co(NO)]^+$ to $[(TPP)Co]^{3+}$, as was earlier reported in the literature.[9]

**FTIR Monitoring of Electrooxidized (TPP)Co(NO).** The infrared spectrum of (TPP)Co(NO) in $CH_2Cl_2$, 0.1 M TBAP is shown in Figure 2. Two strong absorptions are located at 1684 and 1006 $cm^{-1}$. The first is characteristic of bound NO,[3,16] while the second peak is found in all metalloporphyrins.[17,18] There are also relatively low intensity peaks located at 1352 and 1074 $cm^{-1}$. All four peaks are observed in a solid-state spectrum of (TPP)Co(NO), thus suggesting that matrix effects do not present problems in solution studies of this compound.

Figure 3 shows the changes that occur in the FTIR spectrum of (TPP)Co(NO) between 1500 and 1900 $cm^{-1}$ during controlled-potential oxidation at 1.10 V (Figure 3b) and 1.40 V (Figure 3c). The initial electrode reactions at these two potentials are given by eq 1 and 2. Neutral (TPP)Co(NO) has a strong NO

(16) Scheidt, W. R.; Prisse, M. E. *J. Am. Chem. Soc.* **1975**, *97*, 17.
(17) Ercolani, C.; Neri, C.; Sartori, G. *J. Chem. Soc. A* **1968**, 2123.
(18) Ogoshi, H.; Masai, N.; Yoshida, Z.; Takemoto, J.; Nakamoto, K. *Bull. Chem. Soc. Jpn.* **1971**, *44*, 49.

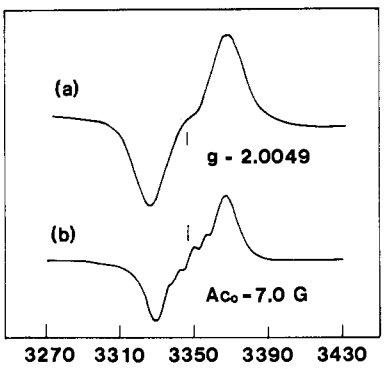


**Figure 4.** ESR spectra of $[(TPP)Co(NO)]^+$ generated by controlled-potential electrolysis of (TPP)Co(NO) in $CH_2Cl_2$, 0.1 M TBAP at 1.10 V: (a) at room temperature; (b) at −150 °C.

absorbance at 1684 $cm^{-1}$ (see Figures 2 and 3a). However, this band disappears as (TPP)Co(NO) is converted to $[(TPP)Co(NO)]^+$ and is replaced by a new NO absorbance at 1726 $cm^{-1}$. This absorbance is assigned to the NO vibration of oxidized $[(TPP)Co(NO)]^+$. Similar assignments for coordinated NO have been reported for neutral and electrooxidized (OEP)Co(NO), (OEC)Co(NO), and (OEiBC)Co(NO) in Nujol mulls.[7]

The NO molecule in $[(TPP)Co(NO)]^{2+}$ remains associated on the microvoltammetric time scale (see Figure 1a) but dissociates from $[(TPP)Co(NO)]^{2+}$ during controlled-potential electrolysis at 1.40 V. This is demonstrated by the negative peak at 1684 $cm^{-1}$ in Figure 3c. Thus, the IR data are consistent with the overall EC type mechanism given by eq 2 and 6.

**ESR Monitoring of (TPP)Co(NO) Electrooxidation in $CH_2Cl_2$.** The location of the unpaired electron in $[(TPP)Co(NO)]^+$ was determined by ESR spectroscopy. Both $A_{1u}$ and $A_{2u}$ porphyrin radicals can be formed in the oxidation process.[19-22] An $A_{1u}$ or $A_{2u}$ state depends on both the axial ligand properties and the degree of saturation of the porphyrin ring.[20,23]

Chang and Fajer[7] studied $[(OEP)Co(NO)]^+$ and its saturated derivatives $[(OEC)Co(NO)]^+$ and $[(OEiBC)Co(NO)]^+$. An $A_{1u}$ radical is reported for the two saturated-ring compounds, but an $A_{2u}$ state was favored for $[(OEP)Co(NO)]^+$. This assignment was based on optical data, since there was no well-defined cobalt coupling in the ESR spectra that would have been definitive in assigning an $A_{1u}$ or an $A_{2u}$ state to the unpaired electron.

ESR spectra of electrogenerated $[(TPP)Co(NO)]^+$ are shown in Figure 4. At room temperature the spectrum has a peak separation $\Delta H_{pp}$ = 41.4 G and a $g$ = 2.0049. A splitting from the central cobalt ion or from the $\beta$ protons of the pyrroles is not observed at room temperature, but the spectrum at −150 °C has a $\Delta H_{pp}$ = 35.7 G and a $g$ = 2.0049. There is a well-resolved splitting from cobalt and a coupling constant of 7.0 G. This large coupling constant indicates a strong interaction between the unpaired electron on the porphyrin ring of $[(TPP)Co(NO)]^+$ and the cobalt nuclei.[7,23] This is in good agreement with the unpaired electron being in the $A_{2u}$ state, which consists of orbitals from the pyrrole nitrogens and the meso-carbons of the porphyrin ring. A large coupling constant is more expected for cobalt porphyrins in an $A_{2u}$ state than for radicals in an $A_{1u}$ state, where the electron density is mainly on the $\alpha$- and $\beta$-carbons of the pyrroles, which are farther removed from the central cobalt atom.[24,25] The measured coupling constant of 7.0 G is in good agreement with that of other $A_{2u}$ cobalt porphyrin radicals in which 6–7-G coupling constants are usually observed.[19,22]

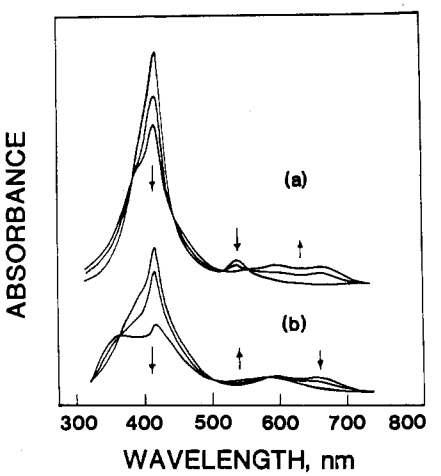


**Figure 5.** Thin-layer UV–visible spectra during oxidation of (TPP)Co(NO) in $CH_2Cl_2$, 0.1 M TBAP at a potential scan rate of 2 mV/s: (a) between 0.00 and 1.13 V; (b) between 1.13 and 1.34 V.

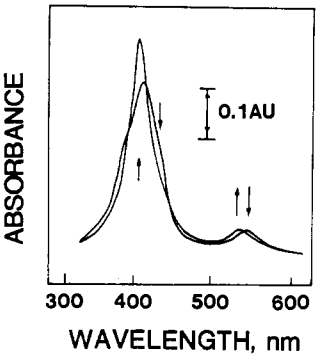


**Figure 6.** Thin-layer UV–visible changes during the first reduction of (TPP)Co(NO) in $CH_2Cl_2$, 0.1 M TBAP. The final product has a spectrum identical with that of $(TPP)Co(CH_2Cl)$.

**Thin-Layer Spectroelectrochemistry of Oxidized (TPP)Co(NO).** UV–visible spectral changes obtained during controlled-potential oxidation of (TPP)Co(NO) in $CH_2Cl_2$ are shown in Figure 5a. Isosbestic points are located at 384, 449, 523, and 553 nm, and the final spectrum indicates that a cation radical is produced during the first oxidation. Spectral changes during the second oxidation of (TPP)Co(NO) are shown in Figure 5b. Isosbestic points are observed at 365, 505, and 595 nm. The final spectrum is similar[15] to that of $[(TPP)Co]^{3+}$. This indicates a dissociation of NO as shown in eq 6 and a further oxidation of $[(TPP)Co]^{2+}$ to give $[(TPP)Co]^{3+}$. Thus, the UV–visible spectral changes are also in good agreement with the FTIR and electrochemical data for this system.

**Electroreduction of (TPP)Co(NO).** (TPP)Co(NO) undergoes two reversible reductions at a microelectrode. Both reductions have the same maximum current height for cyclic voltammetry and for steady-state voltammetry at a microelectrode (see Figure 1a). The first reduction is located at $E_{1/2}$ = −1.18 V in both the conventional and the microelectrode cyclic voltammogram. The second reduction of (TPP)Co(NO) occurs at $E_{1/2}$ = −1.75 V when a microelectrode is utilized and is only present to a small extent in the conventional cyclic voltammogram which has an additional small peak at −1.42 V. This is illustrated in Figure 1b. The peak at −1.42 V does not occur when the reduction of (TPP)Co(NO) is carried out at a microelectrode (see Figure 1a), and this suggests that a chemical reaction occurs after the first reduction. In the case of reduction at a microelectrode, the following chemical reaction does not contribute to the current.[26]

(19) Fajer, J.; Davis, M. S. In *The Porphyrins*; Dolphin, D., Ed.; Academic: New York, 1978; Vol. IV, pp 197–256.
(20) Hanson, L. K.; Chang, C. K.; Davis, M. S.; Fajer, J. *J. Am. Chem. Soc.* **1981**, *103*, 663.
(21) Ohya-Nishiguchi, H.; Khono, M.; Yamamoto, K. *Bull. Chem. Soc. Jpn.* **1981**, *54*, 1923.
(22) Ichimori, K.; Ohya-Nishiguchi, H.; Hirota, N.; Yamamoto, K. *Bull. Chem. Soc. Jpn.* **1985**, *58*, 623.
(23) Anderson, L. A.; Loehr, T. M.; Chang, C. K.; Mauk, G. A. *J. Am. Chem. Soc.* **1985**, *107*, 182.
(24) Fujita, E.; Fajer, j. *J. Am. Chem. Soc.* **1983**, *105*, 6743.
(25) Richardson, P. F.; Chang, C. K.; Spaulding, L. D.; Fajer, J. *J. Am. Chem. Soc.* **1979**, *101*, 7736.
(26) Dayton, M. A.; Brown, J. C.; Stutts, K. J.; Wightman, R. M. *Anal Chem.* **1980**, *52*, 946.

Infrared and UV-visible spectral data show that NO is lost from $[(TPP)Co(NO)]^-$ and that the generated $[(TPP)Co]^-$ reacts with the $CH_2Cl_2$ solvent to give $(TPP)Co(CH_2Cl)$. This reaction has been discussed for the reduction of $(TPP)Co$[27] in $CH_2Cl_2$, and a similar sequence of steps occurs after reduction of (TPP)Co(NO) in $CH_2Cl_2$. The overall conversion of (TPP)Co(NO) to $(TPP)Co(CH_2Cl)$ is given by eq 3, 8, and 9. Similar reactions have

$$[(TPP)Co(NO)]^- \rightarrow [(TPP)Co]^- + NO \quad (8)$$

$$[(TPP)Co]^- + CH_2Cl_2 \rightarrow (TPP)Co(CH_2Cl) + Cl^- \quad (9)$$

also been observed between electrochemically generated $[(TPP)Co]^-$ and alkyl or aryl halides.[28]

Additional proof for the sequence of steps given in reactions 8 and 9 comes from thin-layer spectroelectrochemistry. Spectral changes monitored during controlled-potential reduction of (TPP)Co(NO) are shown in Figure 6. The final spectrum is identical with the UV-visible spectrum of genuine $(TPP)Co(CH_2Cl)$ as well as with other $\sigma$-bonded (TPP)Co(R) complexes in $CH_2Cl_2$.[27-29]

Finally, the difference FTIR spectrum after reduction of (TPP)Co(NO) at -1.30 V shows a negative peak at 1684 $cm^{-1}$, and no characteristic positive band for NO-containing species was observed. This also indicates that NO dissociation has occurred after the first reduction.

In summary, the oxidations and reductions of (TPP)Co(NO) are reversible at a microelectrode, but the ultimate products are not always those shown by eq 1-5. This is due to the extreme reactivity of the singly reduced and doubly oxidized species. It is anticipated that several additional NO complexes may be sufficiently stabilized to be spectroscopically characterized at low temperature, and studies are now being carried out along these lines.

**Acknowledgment.** The support of the National Science Foundation (Grant CHE-8515411) is gratefully acknowledged.

**Registry No.** (TPP)Co(NO), 42034-08-2; $CH_2Cl_2$, 75-09-2; Pt, 7440-06-4; (TPP)Co, 14172-90-8.

(27) Kadish, K. M.; Lin, X. Q.; Han, B. C. *Inorg. Chem.* **1987**, *26*, 4161.
(28) Guilard, R.; Lecomte, C.; Kadish, K. M. *Struct. Bonding (Berlin)* **1987**, *64*, 206-268.
(29) Dolphin, D.; Halko, D. J.; Johnson, E. *Inorg. Chem.* **1981**, *20*, 4384.

Contribution from the Department of Chemistry, Indian Institute of Technology, Madras, India

# Spectroscopic Investigation of Intermolecular Interactions in Dithiolate Complexes of Nickel

S. Lalitha, G. V. R. Chandramouli, and P. T. Manoharan*

*Received May 27, 1987*

A spectroscopic study on maleonitriledithiolato complexes of the type $R_n[M(mnt)_2]$, where $n$ = 1 or 2, M = Ni(II) or Ni(III), and R = $(CH_3)_4N$ or $(n\text{-}C_4H_9)_4N$, is presented. On the basis of the charge potential model, with incorporation of electronegativities, the charges on the various atoms have been calculated by using the binding energies obtained from photoelectron spectroscopic experiments. These are found to compare well with those reported by X$\alpha$ calculations. The binding energy shifts of the atoms on $[(n\text{-}C_4H_9)_4N]_2[Ni(mnt)_2]$ are observed to follow a different trend compared with that in the other three complexes. This difference in the charge distribution in the diamagnetic complex with tetrabutylammonium as the cation has been explained with the help of molecular projections. It has been inferred that there is an interaction between the cation and the complex anion in this case. EPR and Raman spectral studies on this complex at low temperatures (down to 20 K) are reported here. Two phase transitions, which also involve a slight molecular distortion, are detected at 50 and 20 K. Infrared spectra of all these complexes are compared, and this also reveals the same anomalous trend. In order to ascertain this behavior, single-crystal electronic spectra of $[(CH_3)_4N]_2[Ni(mnt)_2]$ at various temperatures are reported.

## Introduction

The remarkable oxidation-reduction behavior of metal dithiolene compounds has generated an intense interest in the synthetic, spectroscopic, and theoretical aspects of these compounds.[1-6] Apart from the interest in these compounds from a purely academic point of view, these systems are now widely employed in industries.[2] One such system widely studied is the maleonitriledithiolate (mnt) complex of transition metals.[3-6] Some of these complexes are, for example, used as an autooxidation catalyst[7] and as a catalyst for the photochemical decomposition of water.[8] A recent paper reports the photoelectrochemical study of some of these complexes.[9]

We have chosen to investigate complexes of the type $R_n^+[M(mnt)_2]^{n-}$, where M = Ni(II), Ni(III), Co(II), Co(III), and Cu(II) and R = $[N(CH_3)_4]$, $[N(C_4H_9)_4]$ (referred to hereafter as $Me_4N$ and $n\text{-}Bu_4N$ respectively), *N*-methylphenazinium, tropilium, etc. by photoelectron spectroscopy, EPR, Raman, optical, and IR spectroscopic techniques. In this paper we present the results pertaining to our study on $R_n^+[Ni(mnt)_2]^{n-}$ complexes, where R = $[N(CH_3)_4]$ and $[N(C_4H_9)_4]$, $n$ = 1 and 2, and M = Ni(II) or Ni(III) in which the complex anion has a planar geometry as shown in Figure 1.

X-ray photoelectron spectroscopy enables a fresh insight into this fairly complex bonding system, since the binding energy (BE) of the core levels of all the atoms can easily be measured and the charges on these atomic sites can be determined. While the BE

(1) McCleverty, J. A. *Prog. Inorg. Chem.* **1968**, *10*, 49.
(2) Burns, R. P.; McAuliff, C. A. *Adv. Inorg. Chem. Radiochem.* **1979**, *22*, 303.
(3) Shupack, S. I.; Billig, E.; Clark, R. J. H.; Williams, R.; Gray, H. B. *J. Am. Chem. Soc.* **1964**, *86*, 4594.
(4) Schrauzer, G. N.; Mayweg, V. P. *J. Am. Chem. Soc.* **1965**, *87*, 3585.
(5) Schmitt, R. D.; Maki, A. H. *J. Am. Chem. Soc.* **1968**, *90*, 2288.
(6) Sano, M.; Adachi, H.; Yamatera, H. *Bull. Chem. Soc. Jpn.* **1981**, *54*, 2636.
(7) Sultin, N.; Yandell, Y. K. *J. Am. Chem. Soc.* **1973**, *95*, 4847.
(8) Henning, R.; Schlamann, W.; Kirsh, H. *Angew. Chem.* **1980**, *92*, 664.
(9) Persaud, L.; Langford, C. H. *Inorg. Chem.* **1985**, *24*, 3562.

0020-1669/88/1327-1492$01.50/0 